

DRL No. 162  
DRL Line Item No. 6

JPL NO. 9950-905

DOE/JPL-956046-83/9  
Distribution Category 4C-63

Annual Report

1484-28221

CARBON, OXYGEN AND THEIR INTERACTION WITH INTRINSIC

POINT DEFECTS IN SOLAR SILICON RIBBON MATERIAL

Annual Report

Period: September, 1982 to September, 1983

JPL CONTRACT NUMBER 956046, Report # 9

Prepared by: U. Gösele and D.G. Ast

Department of Materials Science and Engineering  
Cornell University, Ithaca N.Y. 14853

October 1983

The JPL Low-Cost solar Array Project\* is sponsored by the U.S. Department of Energy and forms part of the Solar Photovoltaic Conversion Program to initiate a major effort towards the development of low-cost solar arrays. This work was performed for the Jet Propulsion Laboratory, California Institute of Technology by the agreement between NASA and DOE.

\*Now known as the Flat Plate Solar Array Project

This report was prepared as an account of work sponsored by the United States Government. Neither the United States nor the United States Department of Energy, nor any of their employees, nor any of their contractors, subcontractors, or their employees, make any warranty, express or implied, or assumes any legal liability or responsibility for the accuracy, completeness or usefulness of any information, apparatus, product or process disclosed, or represents that its use would not infringe privately owned rights.

Carbon, Oxygen and their Interactions with Intrinsic Point Defects  
in Silicon Ribbon Material-

A Speculative Approach

U. Gösele\* and D.G. Ast

Dep. Materials Science and Engineering, Cornell University, Bard Hall,  
Ithaca, N.Y. 14853

Abstract

This report first provides some background information on intrinsic point defects, and on carbon and oxygen in silicon in so far as it may be relevant for the efficiency of solar cells fabricated from EFG ribbon material. We discuss the co-precipitation of carbon and oxygen and especially of carbon and silicon self interstitials. A simple model for the electrical activity of carbon-self-interstitial agglomerates is presented. We assume that the self-interstitial content of these agglomerates determines their electrical activity and that both compressive stresses (high self-interstitial content) and tensile stresses (low self-interstitial content) give rise to electrical activity of the agglomerates. The self-interstitial content of these carbon-related agglomerates may be reduced by an appropriate high-temperature treatment and enhanced by a supersaturation of self-interstitials generated during formation of the p-n junction of solar cells.

It is suggested that oxygen present in supersaturation in carbon-rich silicon may be induced to form  $\text{SiO}_2$  precipitates by self-interstitials generated during phosphorus diffusion. It is proposed that the  $\text{SiO}_2$ -Si interface of the precipitates gives rise to a continuum of donor states and that these interface states are responsible for at least part of the light-enhancement effects observed in oxygen containing EFG silicon after phosphorus diffusion.

\*Permanent address: Max-Planck-Institut für Metallforschung, D-7000 Stuttgart 80, West Germany.

## 1. Introduction

Silicon ribbon material grown by the edge-defined film-fed growth (EFG) technique invariably contains a high concentration of carbon, about  $10^{18}\text{cm}^{-3}$ . The carbon is introduced by the slotted graphite die in which liquid silicon rises by capillary action. Silicon solidifying above the die

is withdrawn in the form of a thin continuous ribbon. EFG ribbons usually exhibit a much smaller minority carrier diffusion length  $L_D$  (typically in the order of 10-50  $\mu\text{m}$ ) and also a correspondingly lower minority carrier life time than float-zone grown (FZ) silicon or Czochralski-grown (CZ) silicon. Recently it has been suggested that the presence of carbon-point defect agglomerates may be at least partially responsible for low  $L_D$  values in EFG ribbons.<sup>1</sup> Other and more commonly involved causes for low  $L_D$  values in EFG ribbons are the presence of a comparatively high density of crystallographic defects, such as various types of grain boundaries and dislocations (both in a very inhomogeneous distribution), as well as contamination with metallic impurities. Grain boundaries in EFG ribbons can be excluded as the main cause for low  $L_D$  values, because the average distance between electrically active grain boundaries is usually in the order of hundreds of  $\mu\text{m}$  and therefore much exceeds  $L_D$ . Therefore, we are left with a "diffusion-length triangle", see Fig. 1, with the remaining three possible causes for the low  $L_D$  values in EFG ribbons (dislocations, metallic impurities, and point-defect-carbon agglomerates) denoted at each corner. These three types of defects may influence each other (e.g., dislocations may absorb point defects; point-defect agglomerates and dislocations may act as gettering centers for metallic impurities; metallic impurity precipitates may act as nucleation sites for point-defect agglomerates; etc) and in different areas of the

ribbons different types of defects may be responsible for a low  $L_D$  value.

The influence of metallic impurities and of dislocations on  $L_D$  has been treated in other publications. We therefore concentrate in the present report on the possibility of a diffusion-length limitation by point-defect-carbon agglomerates. The report is by no means meant to be complete or to provide final answers. It is rather our intention to stimulate more specific experimental investigations by proposing some speculations and also a very rough model for understanding at least qualitatively the change of  $L_D$  by various treatments of the ribbons, such as high temperature heat treatments of phosphorus diffusion steps. Since our model is based on interactions between intrinsic point defects and carbon and oxygen in silicon we will first compile some basic information on intrinsic point defects (Section 2) and on carbon and oxygen in silicon (Section 3) which is required to understand and to develop our model in some detail in the subsequent sections. Readers who are familiar with point defects and carbon and oxygen in silicon may directly proceed to Section 4.

## 2. Some basic information on point defects in silicon.

### 2.1. Point defects and diffusion under thermal equilibrium conditions.

A perfect crystal can decrease its Gibbs free energy by introducing a certain concentration of point defects into the crystal. For a crystal consisting of one element, like silicon, two basic types of point defects have to be considered, namely vacancies,  $V$ , (one silicon atom missing) and

self-interstitials, I, (one extra silicon atom squeezed into the crystal) as schematically shown in Fig. 2. In Fig. 2, we have also indicated chemical point defects, such as substitutional dopants and foreign interstitial atoms, such as most metallics in silicon. The thermal equilibrium concentrations (in dimensionless atomic fractions) of vacancies,  $C_V^{eq}$ , and of self interstitials,  $C_I^{eq}$ , are given by

$$C_V^{eq} = \exp (S_V^F/k) \exp (-H_V^F/kT) \quad (1)$$

$$C_I^{eq} = \exp (S_I^F/k) \exp (-H_I^F/kT) \quad (2)$$

where  $k$  is Boltmann's constant and  $T$  the absolute temperature.  $S_V^F$  and  $H_V^F$  are the entropy and the enthalpy of formation of a vacancy, respectively.  $S_I^F$  and  $H_I^F$  are the corresponding quantities for self-interstitials.

Although in the literature various values can be found for  $H_V^F$ , these quantities have not yet been determined experimentally, basically because the concentrations of vacancies or self-interstitials are very low ( $< 10^{16} \text{cm}^{-3}$ ) even at the melting point. In the literature there exists a long standing controversy whether self-interstitials are present at all in silicon in quantities comparable to vacancies.<sup>2</sup> In the following we take the view that vacancies and self-interstitials co-exist in silicon<sup>59</sup> and have to be taken into account for understanding diffusion processes in silicon. (Gösele and Tan<sup>3</sup>, Frank et al.<sup>4</sup>). Whereas hardly anything reliable is known on  $C_V^{eq}$  and  $C_I^{eq}$ , the situation is different for the basic silicon material transport quantity, namely the self-diffusion coefficient  $D^{SD}$ , which is given by

$$D^{SD} = D_V C_V^{eq} + D_I C_I^{eq} \quad (3)$$

where  $D_V$  and  $D_I$  are the diffusion coefficients of vacancies and self-interstitials, respectively. The individual terms in (3) are given by 3,4

$$D_V C_V^{eq} = 0.57 \exp(-4.03 \text{ eV}/kT) \text{ cm}^2 \text{ s}^{-1} \quad (4)$$

$$D_I C_I^{eq} = 914 \exp(-4.84 \text{ eV}/kT) \text{ cm}^2 \text{ s}^{-1}, \quad (5)$$

as also shown in Fig. 3.

The individual diffusivities  $D_V$  and  $D_I$  are as poorly known as the concentrations  $C_V^{eq}$  and  $C_I^{eq}$ . We, nevertheless, present in Fig. 4 and Fig. 5 recent rough estimates of these quantities by Gösele and Tan<sup>5</sup>, but remind the reader that this information has been reached very indirectly and may have to be revised considerably in the future. We mention explicitly that the quantities expressed in (1-5) hold for intrinsic silicon and depend on the position of the Fermi level.

## 2.2 Interaction between vacancies and self-interstitials

If both vacancies and self-interstitials are present in silicon it can be expected that they react with each other according to the reaction



where 0 represents the undisturbed silicon lattice. This reaction, which for silicon has first been proposed by Prussin<sup>6</sup> and later on more specifically by Sirtl<sup>7</sup>, involves the recombination of I and V as well as the spontaneous thermal creation of I and V pairs (Frenkel pairs) in the silicon lattice. If the point defect concentrations are disturbed by some external means (e.g. by surface oxidation, which injects interstitials into the silicon) then for sufficiently long times reaction (6) will establish a local dynamical equilibrium between I and V which may be described by the law of mass action as 3,7

$$C_I C_V = C_I^{eq} C_V^{eq} \quad (7)$$

In eq. (7)  $C_I$  and  $C_V$  are the actual concentrations of self-interstitials and vacancies, and  $C_I^{eq}$  and  $C_V^{eq}$  their respective thermal equilibrium values. Measurements of Antoniadis and Moskowitz<sup>8</sup> showed that at 1100° C it takes a time

$$T_{dyn} (1100^\circ\text{C}) \approx 1 \text{ hr} \quad (8)$$

to reach local dynamical equilibrium conditions described by (7). It has been estimated<sup>4</sup> that  $T_{dyn}$  should increase with decreasing temperatures approximately inversely proportional to the silicon self-diffusion coefficient  $D^{SD}$ . For 900° C this leads to the estimate:

$$T_{dyn}(900^\circ\text{C}) \approx \text{days}, \quad (9)$$

which means in practical terms, that for experiments performed at 900° C at much shorter times (e.g. a 30 min phosphorus diffusion) the vacancies and

self-interstitials can be treated as non-interacting species.

### 2.3 Diffusion of substitutional elements

The diffusion of substitutional elements in silicon (such as Group-III or Group-V dopants, substitutional carbon, or as a special case, silicon atoms themselves) requires intrinsic point defects. Under thermal equilibrium conditions, their diffusivity  $D^S$  is composed of a contribution  $D_V^S$  involving vacancies and a contribution  $D_I^S$  involving self-interstitials as "diffusion vehicles" according to<sup>3,4,8,9</sup>

$$D^S = D_I^S + D_V^S \quad (10)$$

The relative vacancy and self-interstitial contributions depend on the specific element and on temperature. Generally, atoms smaller than silicon, such as boron or phosphorus show an essential relative contribution  $D_I^S/D^S$  of the diffusion component involving self-interstitials. It has been argued<sup>3</sup> that carbon which is very much smaller than silicon should also diffuse predominantly via a diffusion process involving self-interstitials; (see also Section 3.2).

If the point defect concentrations are disturbed by external means (e.g. oxidation, P-diffusion) and attain values  $C_V$  and  $C_I$  then the diffusivity  $D^S$  of a substitutional element is changed to<sup>3,4,8</sup>

$$D_{\text{ext}}^S \approx D_I^S(C_I/C_I^{\text{eq}}) + D_V^S(C_V/C_V^{\text{eq}}) \quad (11)$$

At high temperatures and sufficiently long times  $C_I$  and  $C_V$  are related via (7). At lower temperatures and not too long times  $C_I$  and  $C_V$  may be regarded as independent of each other, as explained in the previous subsection.

#### 2.4 Generation of non-equilibrium concentrations of intrinsic point defects

There exist various possibilities to change point defect concentrations from their thermal equilibrium values  $C_I^{eq}$  and  $C_V^{eq}$  to some other values  $C_I$  and  $C_V$ , respectively. In this subsection we do not consider particle irradiation in which the same numbers of vacancies and self-interstitials are generated, but rather surface treatments such as oxidation or the in-diffusion of phosphorus from the surface. In the subsequent subsection we will also mention non-equilibrium situations related to the crystal growth process.

Surface oxidation of silicon leads to the formation and growth of an amorphous  $SiO_2$  film on top of the silicon. The  $SiO_2$  film growth leads to the injection of silicon self-interstitials <sup>3,8,9</sup> into the silicon crystal giving rise to  $C_I > C_I^{eq}$ . The resulting supersaturation of self-interstitials,

$$s_I = (C_I - C_I^{eq}) / C_I^{eq} \quad (12)$$

depends on surface orientation, and on the detailed composition of the atmosphere and on temperature. For (100) surface orientation in dry oxygen one obtains approximately <sup>10</sup>

$$s_I = 6.6 \times 10^{-9} t^{1/4} \exp(2.53 \text{ eV}/kT) s^{1/4}, \quad (13)$$

which means that  $s_I$  strongly decreases with increasing temperatures. For (111) surfaces the right-hand side has to be multiplied by a factor of about 0.6. For wet oxidation multiplication factors larger than unity have to be applied.<sup>11</sup> For high temperatures and long times (e.g., for  $t \geq 1$  hour at 1100°C) the oxidation induced self-interstitial supersaturation ( $C_I > C_I^{eq}$ ) is related to a vacancy undersaturation ( $C_V < C_V^{eq}$ ) according to eq. (7). Oxidation-induced self-interstitials may agglomerate and form interstitial-type stacking faults, so called Oxidation induced Stacking Faults, or in short, OSF. Oxidation-induced self-interstitials also leads also lead to enhanced diffusion (see eq. 11) of substitutional elements with a sufficiently high diffusion component involving self-interstitials (e.g., B, P, Al, Ga, In, and to a smaller extent, As) and to retarded diffusion of substitutional elements which prefer to migrate via a vacancy mechanism (e.g., Sb)<sup>12</sup>.

The addition of a chlorine-containing compound in the oxidizing atmosphere (e.g., HCl, Cl<sub>2</sub>) may lead to the injection of vacancies into the crystalline silicon<sup>13,14</sup>. An example for this effect in terms of  $s_I$  is shown in Fig. 6 as a function of the HCl content of the atmosphere at 1200°C. A negative value of  $s_I$  (a self-interstitial undersaturation) corresponds to a vacancy supersaturation.

The diffusion of phosphorus into silicon starting from a high surface concentration creates a supersaturation of intrinsic point defects which diffuse into the silicon.<sup>20</sup> This supersaturation gives rise to enhanced diffusion of substitutional dopants in front of the in-diffusing phosphorus

leading to the well-known "emitter-push effect" and to the broadening of so-called marked layers,<sup>20</sup> see Fig. 7. This supersaturation also leads to the climb of dislocations. Screw dislocation will turn into helices; an example is shown in Fig. 8. Analysis of the climb direction of such helices<sup>21</sup> and also of dislocation loops<sup>22</sup> showed that phosphorus generates a supersaturation of self-interstitials. This supersaturation strongly decreases with increasing temperature.<sup>23</sup> At 900°C  $C_I/C_I^{eq}$  can be well above 100. If there are no sinks for self-interstitials in the silicon bulk then the phosphorus-generated self-interstitials may diffuse very deep into the silicon, e.g., for 30 minutes (of phosphorus diffusion) at 900°C, (a typical situation in solar cell processing) the self-interstitial may diffuse about 100  $\mu\text{m}$  into the silicon.<sup>24</sup> The actual range depends on the concentration of sinks, (e.g. dislocations) in the silicon. A high dislocation density will limit the self-interstitial supersaturation to a region of a few microns near the surface. The effect of dislocations on the range of the supersaturation will be discussed in more detail in subsection 2.6.

If helical dislocations are found in phosphorus diffused silicon the point-defect supersaturation may conveniently be estimated from the number of turns per length,  $N_L$ , via the formula<sup>25</sup>:

$$\ln(C_I/C_I^{eq}) \approx 2\pi N_L G b^4 / kT, \quad (14)$$

where  $b$  is the length of the Burgers vector and  $G$  the shear modulus.  $T$  is the absolute temperature at which the helical dislocations were formed.

## 2.5 Agglomeration of intrinsic point defects during crystal growth

During the growth of silicon single crystals the crystal is cooled down from the melting temperature to room temperature. Since the point-defect thermal equilibrium concentrations are highest at the melting point the crystal has to get rid of part of this point defect when it cools down. If the rate  $v$  of crystal growth is sufficiently small the point defects may attain their equilibrium values for the lower temperatures by the diffusion of excess point defects to the surface or back to the melt. For higher growth rates the point defects will form point-defect agglomerates. For silicon basically two types of microdefects which are commonly termed swirl defects, have been detected by Cu decoration or preferential etching: A-swirls and B-swirls.<sup>26</sup> A-swirls have been identified by high-voltage electron microscopy as interstitial-type dislocation loops.<sup>27,28</sup> B-swirls, if not decorated by copper, cannot be seen or identified in an electron microscope. Experimentally it has been found that carbon facilitates the nucleation and extends the range of stability of B-swirl defects.<sup>26,29,30</sup> Although it has never conclusively proven experimentally, we adopt the model of Foll et al.,<sup>29,30</sup> in which it is assumed that B-swirls consist of co-precipitates of carbon and silicon self-interstitials. These carbon-self-interstitial complexes are thought to be able to transform into A-swirl defects. The alternative view that B-swirls are carbon-vacancy complexes is unlikely, at least based on simple volume considerations.

With increasing growth rates first the A-swirls and then the B-swirls disappear. The growth rate value  $v$  where the B-swirls disappear increases with increasing carbon concentration.<sup>26,30</sup> Increasing the growth rate even further, a new type of micro-defects occurs, (see Fig. 10), so-called D-swirls, the nature of which has not yet been identified.<sup>31</sup> It is likely that D-swirls consist of vacancy agglomerates.<sup>32</sup>

In recent years it turned out that it is not the growth rate  $v$  itself, which determines the appearance and disappearance of the various swirl-types but rather the quantity <sup>32,33,34</sup>

$$q = v/G, \quad (15)$$

where  $G = |\Delta T/\Delta Z|$  is the temperature gradient.

Regarding micro-defects in silicon EFG silicon ribbon material the first impression is that none of the concepts for microdefects formation developed for CZ and FZ-single crystals can be applied, basically because the growth rate of ribbons is much higher, the ribbon thickness is very small and the ribbon material contains a high density of dislocations. However, a closer look shows that the situation concerning microdefects may not be very different in EFG ribbon material. Since both  $v$  and the temperature gradient  $G$  are higher by about a factor of ten for EFG ribbons compared to CZ-grown Si crystals, the physically relevant parameter  $q = v/G$  remains in the same order of magnitude. The fact that the thickness of ribbons (about 200-300  $\mu\text{m}$ ) is in the same order of magnitude as the thickness of the swirl-free zone<sup>26-33</sup> near the rim of CZ or FZ-grown Si crystals does not mean that no swirl-like defects could be expected in silicon ribbons at all. The thickness  $d_s$  of the swirl-free zone at the crystal surfaces should be proportional to the cooling time, or in terms of  $v$  and  $G$ :

$$d_s \propto 1/(v G) \quad (16)$$

Since  $v$  and  $G$  are both about a factor of ten larger during ribbon growth, we expect about 100 times smaller denuded zones, for ribbons, in the order of

some  $\mu\text{m}$  at most. A similar consideration also applies to the influence of dislocations. As long as the density of dislocations which can act as sinks for point defects is so that their average distance is 10  $\mu\text{m}$  or more (corresponding to dislocation densities  $< 10^6\text{cm}^{-2}$ ) dislocations are not likely to prevent swirl formation.

Finally we note that EFG silicon ribbons contain a high concentration of carbon which favors the formation of B-swirl defects<sup>29,30</sup>. Taking into account all the various factors concerning crystal growth of EFG ribbons we consider it as likely that these ribbons contain small B-swirls which may be viewed as carbon-rich zones decorated with silicon self-interstitials. The experimental result that no carbon agglomerates or precipitates could be detected with transmission electron microscopy<sup>35</sup> is in line with this assumption, since undecorated B-swirls in FZ or CZ crystals could also not be detected by transmission electron microscopy<sup>26,30</sup>. We suggest to do Cu decoration experiments in order to show the existence of B-swirls in EFG ribbons.

In Section 4 we will present a model for the expected behavior of such carbon-self-interstitial agglomerates under the influence of high temperature heat treatments or phosphorus diffusion steps.

## 2.6 Absorption of point defects by dislocations

Intrinsic point defects present in supersaturation may be absorbed by dislocations. If the absorption is limited by the diffusion of point defects

to dislocations, then the average time  $t_a$  until the supersaturated point defects are absorbed by dislocations of density  $\rho$  is given by

$$t_a \approx 1/(\rho D_{I,V}) \quad (17)$$

where  $D_I$  or  $D_V$  is the diffusivity of the respective diffusing point defects. Eq. (17) may be expressed in a different form as

$$\sqrt{Dt_a} \approx 1/\rho \quad (18)$$

which basically says that the average distance a diffusing point defect can cover before it is absorbed by dislocations is about the average spacing between dislocations. This means, e.g., that a density of dislocations (which are assumed to act as perfect sinks for point defects) of about  $10^6 \text{cm}^{-2}$  will limit a phosphorus-induced supersaturation of self-interstitial to the first  $10 \mu\text{m}$  below the surface.

In the context of dislocations in silicon EFG ribbons the observation of Kastner and Hesse<sup>26</sup> may be of interest, who found that deformation-induced dislocations do not absorb point defects efficiently. A heat treatment at  $1200^\circ\text{C}$  for 1 hour transformed the dislocations into a configuration in which they acted as almost perfect sinks for point-defects. This behavior is most likely related to the fact that dislocations in Si directly after deformation are usually dissociated and get at least partly constricted only after a high temperature treatment.<sup>37</sup> Since most dislocations in EFG ribbons are probably not grown-in from the melt but are introduced during cooling due to high mechanical stresses it is conceivable that part of these deformation-induced

dislocations do not act as efficient point-defect absorbers before an additional high temperature heat treatment.

### 3. Some basic information on carbon and oxygen in silicon

Information on carbon in silicon and its impact on devices is compiled in a recent article by Kolbesen and Muhlbauer.<sup>38</sup> The behavior and the properties of oxygen in silicon have been dealt with in the review articles by Patel<sup>39,40</sup> and by Gösele and Tan.<sup>41</sup> For detailed references we refer to these papers.

#### 3.1 Configurations, solid solubility, electrical inactivity, and influence on lattice parameter

##### 3.1.1 Carbon

Carbon is mainly dissolved on substitutional sites in silicon (Fig. 1, Fig. 11). It is smaller than silicon and leads to a decrease of the lattice constant (see Fig. 12) corresponding to a lattice contraction of about one atomic volume for each carbon atom incorporated.<sup>42</sup> Substitutional carbon is electrically inactive. The solid solubility of carbon in silicon has been measured by Bean and Newman<sup>43</sup> as

$$c_s^{eq} = 4 \times 10^{24} \exp(-2.3\text{eV}/kT) \text{cm}^{-3}, \quad (19)$$

see also Fig. 13. If both carbon and oxygen are present in silicon in high concentrations the concept of a solid solubility becomes rather ill-defined

because of interactions between carbon and oxygen (see for example: Zulehner<sup>44</sup>).

### 3.1.2 Oxygen

Oxygen is incorporated in silicon in a slightly off-centered interstitial position between two neighboring silicon atoms<sup>46-48</sup> as indicated in Fig. 14. Oxygen atoms in this position (denoted as interstitial oxygen  $O_i$ ) is electrically inactive. Its solid solubility in silicon is given by<sup>41,49</sup>:

$$C_I^{eq} = 1.53 \times 10^{21} \exp(-1.03 \text{ eV}/kT) \text{ cm}^{-3}; \quad (20)$$

see also Fig. 13. Because of its incorporation in interstitial position, oxygen, contrary to carbon, leads to an increase of the lattice constant (see Fig. 12).<sup>50</sup>

### 3.2 Diffusion of carbon and oxygen in silicon

Due to its interstitial position oxygen does not require intrinsic point defects for diffusion through the silicon lattice. A diffusive jump of  $O_i$  requires the breaking of a Si-O bond and simultaneously leads to a change of the preferential Si-O-Si axis from one  $\langle 111 \rangle$  direction to another one (Fig. 14). The diffusivity  $D_i$  of interstitial oxygen by this process is given by<sup>48,51,52</sup>

$$D_i = 0.23 \exp(-2.56 \text{ eV}/kT) \text{ cm}^2 \text{ sec}^{-1}, \quad (21)$$

see Fig. 15.

Due to its substitutional position the diffusion of carbon in silicon requires intrinsic point defects. As discussed in Section 2.3 on the diffusion of substitutional elements in silicon the diffusivity of substitutional carbon<sup>53</sup>,

$$D_c = 1.9 \exp(-3.1 \text{ eV}/kT) \text{ cm}^2 \text{ sec}^{-1}, \quad (22)$$

should be composed of a contribution  $D_V^C$  involving vacancies and a contribution  $D_I^C$  involving self-interstitials:

$$D_c = D_I^C + D_V^C \quad (23)$$

Nothing is known experimentally on the ratio  $D_V^C/D_I^C$  but following the arguments of Gosele and Tan<sup>3</sup>, we expect that carbon as a very small substitutional element should show a large component  $D_I^C$  compared to  $D_V^C$  ( $D_I^C \gg D_V^C$ ). A probable diffusion mechanism of substitutional carbon ( $C^S$ ) via self-interstitials (I) involves the formation of a highly mobile carbon-self-interstitial complex (CI) according to



Such a highly mobile carbon-self-interstitial complex has for example been found by Watkins and Brower<sup>54</sup> after low temperature electron irradiation of silicon. The configuration of this complex is shown in Fig. 16.

### 3.3 Influence of intrinsic point defects on carbon and oxygen diffusion in silicon

Following the arguments on the dominant diffusion mode of carbon involving self-interstitials, we expect that a supersaturation of self-interstitials ( $C > C_I^{eq}$ ) should enhance the thermal equilibrium diffusivity  $D_c$  of carbon to a value

$$D_c^{ext} \approx D_c (C_I / C_I^{eq}). \quad (25)$$

As discussed in subsection 2.4 a supersaturation of self-interstitials can be generated by thermal oxidation or by the in-diffusion of phosphorus starting from a high surface concentration. In the case of phosphorus diffusion, say at  $900^\circ\text{C}$ , an enhancement of the carbon diffusivity of up to a factor of 100 can be expected. In the case of a high carbon concentration it has to be taken into account that the phosphorus supplies only a limited amount of self-interstitials and that it may take a finite time until the excess self-interstitials necessary to form the highly mobile  $(CI)$  complexes are formed.

Stavola et al.<sup>52</sup> and Newman et al.<sup>55</sup> have shown experimentally that a supersaturation of self-interstitials may enhance oxygen diffusion at low temperatures ( $< 400^\circ\text{C}$ ), probably by the formation of a highly mobile  $(O_i I)$  complex according to<sup>56</sup>



The main difference to the case of carbon is that the diffusion process according to (26) is a parallel reaction to the normal interstitial oxygen diffusion process and requires very much higher values of  $C_I/C_I^{eq}$  than in the case of substitutional carbon. We therefore expect, that contrary to the case of carbon at high temperatures (say  $>800^\circ\text{C}$ ) oxidation or phosphorus-induced self-interstitials should not appreciably enhance the diffusion of oxygen in silicon.

#### 3.4 Volume considerations concerning oxygen or carbon agglomeration/precipitation

If present in supersaturation ( $C_i > C_i^{eq}$ ) and if the temperature is sufficiently high for them to diffuse, oxygen interstitials will precipitate in the form of amorphous or crystalline  $\text{SiO}_2$  (or an oxide  $\text{SiO}_x$  with  $x$  close to 2). Since the volume  $\Omega_{\text{ox}}$  per  $\text{SiO}_2$  is about twice the atomic volume of silicon in the silicon lattice a corresponding volume increase is associated with  $\text{SiO}_2$  precipitation. Therefore, precipitate growth can proceed only if the silicon matrix is plastically deformed (punching out of dislocation loops) or if for every two oxygen interstitials  $O_i$  incorporated into the precipitate about one silicon self-interstitial is injected into the surrounding silicon matrix\*. The supersaturation of self-interstitials resulting from the latter

\*In principle, the absorption of a vacancy from the silicon matrix is equivalent, provided sufficient vacancies are available in the material. In the following, we will restrict ourselves to a discussion in terms of silicon self-interstitials.

process gives rise to the formation and growth of interstitial-type dislocation loops and extrinsic stacking faults.<sup>40,41,56-58</sup> In Fig. 17 the basic idea for these volume considerations are depicted schematically and compared to the case of carbon agglomeration, where just the opposite volume changes occur.

If carbon is present in a concentration above its solubility limit (19) a thermodynamic driving force will exist for a precipitation process which should lead to the formation of silicon carbide (SiC) provided the interface and stress energies (or an insufficient diffusivity at low temperatures) do not prevent the precipitation. As an alternative to SiC formation a simple agglomeration process of carbon without carbide formation should also be considered. Both processes lead to a local volume contraction of about one atomic volume for each incorporated carbon atom. Therefore growth of the SiC precipitate or the carbon agglomerate can proceed only if for every carbon atom incorporated a self-interstitial is absorbed from the silicon matrix (Fig. 16). This is just the opposite behavior to that of the precipitation of oxygen in silicon.

### 3.5 Co-precipitation of carbon and self-interstitials

In a typical cooling situation after crystal growth silicon self-interstitials are present in supersaturation ( $C_I > C_I^{eq}$ ) and experience a thermodynamic driving force to precipitate. Since in silicon the critical radius for the growth of interstitial-type dislocation loops is fairly high<sup>28</sup> the co-precipitation with carbon in three-dimensional carbon-self-interstitial agglomerates (supposedly the "B-swirls") is a more favorable alternative, provided the carbon concentration is sufficiently high. The volume

considerations described in the previous subsection would indicate a 1:1 ratio of carbon atoms and self-interstitials in the agglomerate. More sophisticated arguments led Foll et al.<sup>28,30</sup> to the assumption that at high temperatures carbon and self-interstitials (in an extended configuration<sup>4,59</sup>) may form a separate phase which may contain a higher percentage of self-interstitials in the agglomerate and which is stable only in the presence of a sufficiently high supersaturation of self-interstitials. Without this supersaturation the self-interstitials will have a tendency to dissociate from the agglomerate and to leave behind a carbon-rich zone.

Within the model of Foll et al.<sup>23,30</sup> B-swirls may collapse and transform in interstitial-type dislocation loops (A-swirls). A similar process may be triggered by a phosphorus-induced supersaturation of self-interstitials. Abe et al.<sup>60</sup> found a high density of stacking faults below phosphorus-diffused areas in carbon-rich material (Fig. 19). This result indicated that carbon or carbon self-interstitial agglomerates may possibly act as nuclei for stacking faults.

### 3.6 Carbon agglomerates as nuclei for SiO<sub>2</sub> precipitates.

It is well established that oxygen in high supersaturation in silicon may form SiO<sub>2</sub> nuclei and precipitate out independent of the presence of carbon in the silicon. For low oxygen supersaturation carbon has been shown to facilitate nucleation of SiO<sub>2</sub> precipitates.<sup>61-66</sup> This behavior is also expected from the simple volume considerations of subsection 3.4: SiO<sub>2</sub> formation leads to an expansion, whereas C agglomeration leads to a contraction of the lattice.

It has experimentally been shown by de Kock<sup>67</sup> that a phosphorus-induced self-interstitial supersaturation leads to  $\text{SiO}_2$  precipitation in regions, where no  $\text{SiO}_2$  precipitation occurred without this supersaturation; see schematic Fig. 19. We assume that the mechanism of facilitating  $\text{SiO}_2$  formation is an indirect one and involves a sufficiently high carbon concentration\*: The P-induced self-interstitials in supersaturation enhance the diffusivity of substitutional carbon according to eq. (25) which in turn facilitates the formation of small carbon-agglomerates, which then will act as nuclei for  $\text{SiO}_2$  precipitates. For more details see ref. 68.

### 3.7 Electrical activity of $\text{SiO}_2$ precipitates

At temperatures around  $450^\circ\text{C}$ , oxygen in silicon forms small agglomerates which act as shallow donors ("thermal donors")<sup>41,46</sup>. Here we are not concerned with these "thermal donors" which may easily be annealed out at temperatures above about  $600^\circ\text{C}$ , but rather with the electrical activity of real  $\text{SiO}_2$  precipitates. It has been found that  $\text{SiO}_2$  precipitates formed between  $600^\circ$  and  $900^\circ\text{C}$  are also electrically active and associated with donor states.<sup>61,69-72</sup> These precipitate-related donors, which show a continuous distribution of states, are commonly termed "new donors" in order to distinguish them from the lower temperature "thermal donors" mentioned above. It is assumed that these donor states are related to the  $\text{SiO}_2$ -Si interface of

\* The carbon concentration of the Si sample used in the experiments has unfortunately not been measured.

the precipitate and probably result from incomplete oxidation (excess silicon) in the  $\text{SiO}_2$  precipitate near the interface. These donor interface states may be destroyed by a high temperature heat treatment which allows the interface to relax and to get rid of excess silicon.

The experimental results on the influence of carbon on these "new donors" may be summarized as follows<sup>61,69,70</sup>: carbon itself is not responsible for the electrical activity, but it is helpful in providing nucleation sites for the  $\text{SiO}_2$  precipitates, the interfaces of which are the real sources of these donor states.

The electrical behavior of these "new donors" is so similar to the centers found in oxygen containing EFG ribbons<sup>73,74</sup> after P-diffusion and showing the so-called "light-enhancement effect"\* that it is very tempting to assume that these oxygen related light enhancement centers are actually nothing else than the "new donors" found in CZ-silicon (see also Sect. 5).

4. A qualitative model for the influence of carbon on the minority carrier diffusion length in EFG ribbons.

\*This means basically that with increasing photon flux the shallow donor states get progressively occupied, so that the electrical activity decreases and the minority carrier diffusion length increases with increasing photon flux (light intensity).

#### 4.1 Basic assumptions

The essentials of our model are contained in the following four assumptions:

- i) As grown carbon-rich EFG silicon ribbons contain a high density  $>10^9\text{cm}^{-3}$ ) of carbon-self-interstitial agglomerates.
- ii) For a given number of carbon atoms in such an agglomerate its electrical activity depends on the content of self-interstitials in the agglomerate. The electrical activity has its minimum (or may be not present at all) for a self-interstitial content corresponding to a basically stress-free state. A higher as well as a lower self-interstitial content leads to stresses at the agglomerate-matrix interface and to a correspondingly higher electrical activity (Fig. 20).
- iii) The self-interstitial content of such agglomerates may be changed by high-temperature heat treatments or by a supersaturation of self-interstitials induced by phosphorus diffusion starting from a high surface concentration. As a reason for a change in the self-interstitial content rather than in the carbon content we invoke the much higher diffusivity of silicon self-interstitials (Fig. 4).
- iv) Increases (decreases) in the electrical activity of these carbon-self-interstitial agglomerates result in correspondingly lower (higher) minority carrier diffusion lengths.

At present, we can prove not even one of these four assumptions. In

the following we will, nevertheless, discuss qualitatively what we expect for various experimental situations in terms of the model based on the above assumptions.

#### 4.2 Influence of a high temperature heat treatment

A heat treatment at say 1200°C for 1 hour changes the microstructure of EFG ribbons. E.g., internal stresses in the ribbons may be minimized by movement of dislocations and their rearrangement into low-angle grain boundaries. We assume that, in addition, the self-interstitial content of grown-in carbon-self-interstitial agglomerates is decreased by dissociation of self-interstitials from the agglomerates and their subsequent diffusion to self-interstitial sinks, such as surfaces or dislocations. If we suppose that we start at the beginning of the heat treatment somewhere near the minimum electrical activity, then we expect to move to the left-hand side in Fig. 20 and to get a decreased diffusion length  $L_D$ , as experimentally observed.<sup>75</sup>

A possible side-effect of such a high-temperature heat treatment is probably that dislocations which have been introduced by plastic deformation during the cooling process after crystal growth increase their ability to absorb intrinsic point defects as discussed in subsection 2.6.

#### 4.3 Interaction with metallic impurities ("Gleichmann Effect").

The carbon-rich zones produced during a high temperature heat treatment, as described in the previous subsection, are likely to act as gettering

centers for metallic impurities. R. Gleichmann<sup>76</sup> suggested that these submicroscopic agglomerates could possibly getter metallic impurities even more effectively than dislocation or high-angle grain boundary. This effect could explain why Gleichmann<sup>76</sup> finds a much lower electrical activity (measured by EBIC) after a one hour 1200°C heat treatment than before the heat treatment: the metallic impurities which had decorated the dislocations before the heat treatment are redistributed to the carbon-rich zones during the heat treatment. It is an essential assumption in this context that the metallic impurities should, on the average, show a lower electrical activity when gettered in carbon-rich zones compared to the case when they decorate dislocations or grain boundaries.

#### 4.4 Influence of Phosphorus Diffusion

Phosphorus diffusion starting from a high surface concentration, as generally used for producing the electrical p-n junction of a solar cell, generates a high supersaturation of silicon self-interstitials as discussed in subsection 2.4. Due to the high density of dislocations, which may act as sinks for self-interstitials, it can be expected that this high supersaturation is restricted to some  $\mu\text{m}$  near the phosphorus-diffused surface. The presence of a high supersaturation of intrinsic point defects in 900°C phosphorus-diffused EFG ribbons can be also concluded from the electron microscopical observation of helical dislocations in the surface near region.<sup>35,76</sup> The supersaturation  $C_I/C_I^{\text{eq}}$  calculated from the number  $n_L$  of turns per unit length of such helices via eq (14) is in the order of 100-500, which can be expected for this kind of phosphorus diffusion at 900°C.

Concerning the carbon-self-interstitial agglomerates, we assume that the high self-interstitial supersaturation will lead to an additional decoration of these agglomerates with self-interstitials. This means in Fig. 20 we move along the electrical activity curve from the left to the right. Suppose, we start near the minimum electrical activity, then during phosphorus diffusion the electrical activity will increase and the minority carrier diffusion length will decrease as often observed after a 900°C 30 min P-diffusion.<sup>75</sup> The situation is different if a high temperature heat treatment (e.g. 1 hr at 1200° C) precedes the phosphorus diffusion, since then due to the high temperature treatment, we are likely to start to the left side of the minimum with a very small self interstitial content. In this case, the phosphorus diffusion will decrease the electrical activity (at least as long as the diffusion times are not excessive) and increase the minority carrier diffusion length as actually observed.<sup>75</sup>

Phosphorus diffusion at higher temperatures than 900°C, say at 1050°C, produces a much lower self-interstitial supersaturation. Under these circumstances it can be expected that the interstitial content of the carbon-self-interstitial agglomerates cannot exceed a certain maximum value which should be lower than the corresponding maximum value for 900°C.

##### 5. Self-interstitial induced oxygen precipitation in carbon-rich EFG ribbons

It has been shown that phosphorus diffusion at 900°C for 30 minutes generates light-enhancement centers in EFG ribbons containing intermediate oxygen concentrations (several times  $10^{17}\text{cm}^{-3}$ ).<sup>73,74</sup> We suppose that these light enhancement centers are due to submicroscopic oxygen precipitates or

basically the "new donors" discussed in subsection 3.7. Probably the nucleation of these  $\text{SiO}_2$  precipitates does not occur throughout the whole ribbons since the oxygen supersaturation is too low at  $900^\circ\text{C}$ . The nucleation obviously needs the triggering by phosphorus-induced silicon self-interstitials as also described in subsection 3.7. Since this self-interstitial supersaturation is present only in a surface-near zone it can be expected that these light-enhancement centers are formed only in this surface-near region (whithin a few  $\mu\text{m}$  of the surface) as is actually the case.<sup>74</sup> This is different in oxygen-rich CZ crystals in which nucleation and growth of oxygen precipitates constituting the light enhancement centers may occur throughout the whole sample. The observation that no oxygen-related light-enhancement centers are formed any more at  $1050^\circ\text{C}$ <sup>75</sup> is probably simply due to the fact that at this temperature the oxygen is no longer (or at least not sufficiently) supersaturated.

## 6. Final remarks

The speculative model presented for the influence of carbon on the minority carrier diffusion length in EFG ribbons certainly so far lacks experimental justification. The most important step would be to render visible the carbon-self-interstitial agglomerates. We suggest that copper decoration and subsequent X-ray topography would constitute a reasonable approach, in view of the fact that carbon-related B-swirls have also been detected this way.<sup>26</sup> The self-interstitial supersaturaton generated by the diffusion of phosphorus also plays an important role in our model. If phosphorus as an n-type dopant were replaced by arsenic then we expect that no increase in the self-interstitial content of carbon-self-interstitial

agglomerates would occur during diffusion (because As does not produce a supersaturation of self-interstitials) and all effects related to this process should disappear. Finally we mention again, that EFG ribbons are so inhomogeneous in their microstructure that we can well imagine that there may also exist regions, where the minority carrier diffusion length is not determined by carbon-self-interstitial agglomerates but rather by dislocations or metallic impurities as indicated in the "diffusion-length triangle" of Fig.

1.

## References

1. J.P. Kalejs and L.A. Ladd, unpublished ("Carbon microdefect influence on high temperature annealing behavior of EFG silicon ribbon").
2. See E.G.: J.A. Van Vechten, in: Handbook of Semiconductors, Vol.3, ed. by S.P. Keller (North-Holland, New York 1980) p.1.
3. U. Gösele and T.Y. Tan, in: Aggregation Phenomena of Point Defects in Silicon, Ed. by E. Sirtl and E. Gorrissen (Electrochem. Soc., Pennington, 1983) p. 17.
4. W. Frank, U. Gösele, H. Mehrer, and A. Seeger, to be published in: Diffusion in Solids II, ed. by A.S. Nowick and G. Murch (Academic Press).
5. U. Gösele and T.Y. Tan, unpublished.
6. S. Prussin, J. Appl. Phys. 43, 2850 (1972).
7. E. Sirtl, in: Semiconductor Silicon 1977, ed. by H.R. Huff and E. Sirtl (Electrochem. Soc., Princeton, 1977) p. 4.
8. D.A. Antoniadis and I. Moskowitz, J. Appl. Phys. 53, 6788 (1982).
9. S.M.Hu, J. Appl. Phys. 45, 1567 (1974).
10. T.Y. Tan and U. Gösele, Appl. Phys. Lett. 39, 86 (1981).

11. B. Leroy, J. Appl. Phys. 50, 7996 (1979).
12. S. Mizuo and H. Higuchi, Jap. J. Appl. Phys. 20, 739 (1981).
13. H. Shiraki, Jap. J. Appl. Phys. 15, 1 (1976).
14. T.Y. Tan and U. Gösele, J. Appl. Phys. 53, 4767 (1982).
15. U. Gösele and T.Y. Tan, in: Defects in Semiconductors, ed. by J.W. Corbett and S. Mahajan (North-Holland, New York, 1983) p. 2.
16. N.A. Stolwijk, B. Schuster, J. Holzl, H. Mehrer, and W. Frank, Physica 116B, 335 (1983).
17. F. Morehead, N.A. Stolwijk, W. Meyberg, and U. Gösele, Appl. Phys. Lett. 42, 690 (1983).
18. W.R. Wilcox, T.J. LaChapelle, and D.H. Forbes, J. Electrochem. Soc. 111, 1377 (1964).
19. H. Kitagawa, K. Hashimoto, and M. Yoshida, Jap. J. Appl. Phys. 20, 2033 (1981).
20. A.F.W. Willoughby, in: Impurity Doping Processes in Silicon, ed. by F.F.Y. Wang (North-Holland, New York 1982) p. 1.
21. H. Strunk, U. Gösele, and B.O. Kolbesen, Appl. Phys. Lett. 34, 530 (1979).

22. R.J. Jaccodine, in ref. 15, p.?
23. R.B.Fair and J.C.C. Tsai, J. Electrochem, Soc. 124, 1107 (1977).
24. D. Lecrosnier, M. Gauneau, J. Paugam, G. Pelous, F. Richou, and P. Henoc, Appl. Phys. Lett. 34, 224 (1979).
25. J. Weertman, Phys. Rev. 107, 1259 (1957).
26. For references, see: A.J.R. de Kock, in ref. 2, p. 247.
27. H. Foll and B.O. Kolbesen, Appl. Phys. 8, 117 (1975).
28. P.M. Petroff and A.J.R. de Kock, J. Cryst. Growth 30, 117 (1975).
29. H. Foll, U. Gösele, and B.O. Kolbesen, J. Crystal Growth 40, 90 (1977); 52, 907 (1981).
30. H. Foll, U. Gösele, and B.O. Kolbesen, in ref. 7, p. 565.
31. P.F. Roksnoer and M.M.B. Van der Boom, J. Cryst. Growth 53, 563 (1981).
32. T. Abe, H. Harada, and J. Chikawa, Physica 116B, 139 (1983).
33. V.V. Voronkov, J. Cryst. Growth 59, 625 (1982).
34. T.Y. Tan, F. Morehead, and U. Gösele, Electrochem. Soc. Spring

Meeting, San Francisco, 1983 (Symposium on Defects in Silicon), to be published.

35. See reports of B. Cunningham and D.G. Ast on "Defect Structure of EFG Ribbons" (1981/1982).
36. S. Kastner and J. Hesse, Phys. Stat. Sol. (a) 25, 261 (1974).
37. J.L.F. Ray and D.J.H. Cockayne, Proc. Roy. Soc. A325, 543 (1971).
38. B.O. Kolbesen and A. Muhlbauer, Solid-State Electronics 25, 759 (1982).
39. J.R. Patel, in: Semiconductor Silicon 1981, ed. by H.R. Huff, R.J. Kriegler, and Y. Takeishi (Electrochem. So., Pennington, 1981) p. 189.
40. J.R. Patel, in ref. 7, p. 521.
41. U. Gösele and T.Y. Tan, Appl. Phys. A28, 79 (1982).
42. J.A. Baker, T.N. Tucker, N.E. Moyer, and R.C. Buscher, J. Appl. Phys. 39, 4365 (1968).
43. A.R. Beau and R.C. Newman, J. Phys. Chem. Solids 32, 1211 (1971).
44. W. Zulehner, in ref. 3, p. 89.
45. A.J.R. de Kock, P.J. Roksnoer, and P.G.T. Boonen, J. Cryst. Growth 22, 311 (1974).

46. W. Kaiser, Phys. Rev. 105, 1751 (1957).
47. C. Hass, J. Phys. Chem. Solids 15, 108 (1960).
48. J.W. Corbett, R.S. McDonald, and G.D. Watkins, J. Phys. Chem. Solids 25, 873 (1964).
49. R.A. Craven, in ref. 39, p. 254.
50. Y. Takano and M. Maki, in: Semiconductor Silicon 1973, ed. by H.R. Huff and R.R. Burgess (Electrochem. Soc., Princeton, 1973) p. 469.
51. J.C. Mikkelsen, Appl. Phys. Lett. 40, 336 (1982).
52. M. Stavola, J.R. Patel, L.C. Kimerling, and P.E. Freeland, Appl. Phys. Lett. 42, 73 (1983).
53. R.C. Newman and J. Wakefield, in: Metallurgy of Semiconductor Materials, Vol. 15, ed by J.B. Schroeder (Interscience, New York, 1961) p. 201, J. Phys. Chem. Solids 19, 230 (1961).
54. G.D. Watkins and K.L. Brower, Phys. Rev. Lett. 36, 1329 (1976).
55. R.C. Newman, J.H. Tucker, and F.M. Livingstone, J. Phys. C., Solid State Phys. 16, L151 (1983).
56. U. Gösele and T.Y. Tan, in ref. 15, p?.

57. S. Mahajan, G.A. Rozgonyi, and D. Brasen, Appl. Phys. Lett. 30, 73 (1977).
58. K. Tempelhoff, F. Spiegelberg, and R. Gleidemann, in ref. 7, p. 585.
59. A. Seeger and K.P. Chik, Phys. Stat. Solidi 29, 455 (1968).
60. T. Abe, K. Kikuchi. S. Shirai, and S. Muraoka, in ref. 39, p. 54.
61. J. Lerouelle, Phys. Stat. Solidi (a) 67, 177 (1981).
62. J. Kishino, Y. Matsushita, and M. Kanamori, Appl Phys. Lett. 35, 213 (1979).
63. S. Kishino, M. Kanamori, N. Yoshihiro, M. Tajima, and T. Iizuka, J. Appl. Phys. 50, 8240 (1979).
64. F. Shimura, H. Tsuya, and T. Kawamura, Appl. Phys. Lett. 37, 483 (1980).
65. R.J. Pinizetto and H.F. Schaake, in Defects in Semiconductors, ed. by J. Narayan and T.Y. Tan (North-Holland, New York, 1981) p. 387.
66. Y. Matsushita, J. Cryst. Growth 56, 516 (1982).
67. A.J.R. De Kock, in ref. 3, p. 58.
68. U. Gösele and D.G. Ast, SRC report "The Influence of Intrinsic Point

Defects on Oxygen Precipitation in Silicon - A Suggestion for the Role of Carbon".

69. V. Cazcarra and P. Zunino, J. Appl. Phys. 51, 4206 (1980).
70. A. Kanamori and M. Kanamori, J. Appl. Phys. 50, 8095 (1979).
71. P.M. Grinshtein, G.V. Lazareva, E.V. Orlova, Z.A. Sal'nik, and V.I. Fistul, Sov. Phys. Semiconductors 12, 68 (1978).
72. M. Tajima, T. Masui, T. Abe, and T. Iizuka, in ref. 39, p. 72.
73. See e.g. C.T. Ho and F.V. Wald, Phys. Stat. Sol. (a) 67, 103 (1981).
74. J.P. Kalejs and L.A. Ladd, unpublished ("Origin of Light Enhancement in Silicon").
75. J.P. Kalejs, private communication.
76. R. Gleichmann; private communication.

## Figure Captions

Figure 1: Main factors likely to influence the minority carrier diffusion length  $L_D$  in EFG ribbons (diffusion length triangle)

Figure 2: Point defects in silicon (schematically)

Figure 3: Self-interstitial ( $D_I C_I^{eq}$ ) and vacancy ( $D_V C_V^{eq}$ ) contribution to silicon self-diffusion according to Gösele and Tan.<sup>15</sup> Experimental data points from references [ 16 - 19 ].

Figure 4: Crude estimate of vacancy ( $D_V$ ) and self-interstitial ( $D_I$ ) diffusivities compared to other diffusivities in silicon.<sup>5</sup> The uncertainty of the values of  $D_I$  and  $D_V$  is at least of the order of a factor of ten.

Figure 5: Crude estimate of thermal equilibrium concentrations of vacancies ( $C_V^{eq}$ ) and of self-interstitials ( $C_I^{eq}$ ).<sup>5</sup> The uncertainty of the individual values is at least of the order of a factor of ten.

Figure 6: Self-interstitial supersaturation  $S_I = (C_I - C_I^{eq})/C_I^{eq}$  as a function of HCl content in an oxidizing atmosphere at 1200°C. Negative values of  $S_I$  corresponds to a vacancy supersaturation.<sup>14</sup>

Figure 7: a) Emitter-push effect

b) broadening of a masked layer due to phosphorus-induced

point-defect supersaturation (schematically).

Figure 8: Transmission electron microscope picture of a helical dislocation, which had formed below a phosphorus-diffused area. (Strunk et al<sup>21</sup>)

Figure 9: The concentration of A-type and B-type swirls in Fz silicon crystals versus growth rate (deKock, Rohsner and Boone<sup>45</sup>; Rohsner and Van den Boom<sup>31</sup>). The physical relevant parameter is not the growth rate  $v$  itself, but rather the combination  $v/G$ , where  $G \sim |\Delta T / \Delta x|$  is the temperature gradient.

Figure 10: Carbon in substitutional position in silicon (schematically)

Figure 11: Normalized change of lattice constant  $d$  of silicon due to substitutional carbon ( $C_s$ ) or interstitial oxygen ( $O_i$ ) (according to references 42 and 50).

Figure 12: Solid solubilities of substitutional carbon ( $C_s$ ) and of interstitial oxygen ( $O_i$ ) in silicon according to Beau and Newman<sup>43</sup> and Craven<sup>49</sup>.

Figure 13: Bond centered configuration of the oxygen interstitial in the silicon lattice. The numbers 1 - 6 note equivalent positions of the oxygen atom. A possible diffusion jump of the oxygen interstitial is indicated (according to Kaiser<sup>46</sup>, Hass<sup>47</sup> and Corbett et al<sup>48</sup>).

Figure 14: Diffusivity of substitutional carbon ( $C_s$ )<sup>53</sup> and of interstitial oxygen ( $O_i$ )<sup>49,51,52</sup> in silicon as a function of reciprocal temperature, compared to silicon self-diffusion ( $S_i$ ), phosphorus diffusion and to the diffusion of interstitial copper ( $C_i$ ).

Figure 15: Configuration of the highly mobile carbon-self-interstitial complex (migration energy 0.9ev) found by Waters and Brower<sup>54</sup> after low temperature electron irradiation.

Figure 16: Volume considerations concerning the formation of  $SiO_2$  precipitates, SiC precipitates or carbon agglomerates.

Figure 17: Formation of stacking faults in carbon-rich silicon by phosphorus induced self-interstitial supersaturation (Abe et al<sup>60</sup>)

Figure 18: Effect of increased nucleation of  $SiO_2$  precipitation by a phosphorus-induced supersaturation of self-interstitials (schematically, de Kock<sup>67</sup>). The carbon concentration of the sample is not known.

Figure 20: Suggested electrical activity of carbon-self-interstitial agglomerates as a function of the self-interstitial content. The minimum electrical activity is expected for a stress-free configuration. It is also indicated by arrows in which direction the self-interstitial content shifts during a high temperature heat treatment or during phosphorus diffusion.

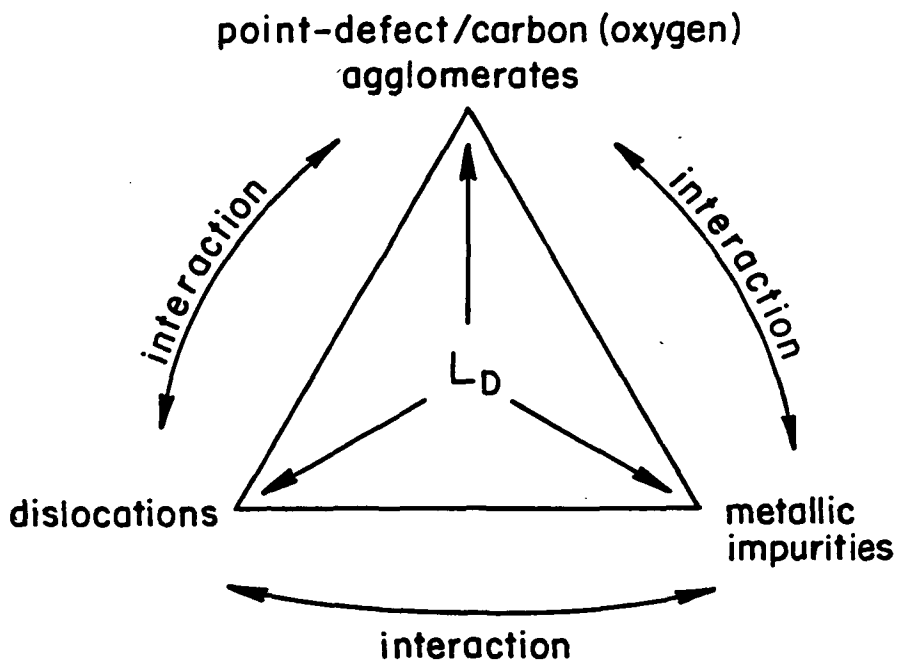


Fig. 1

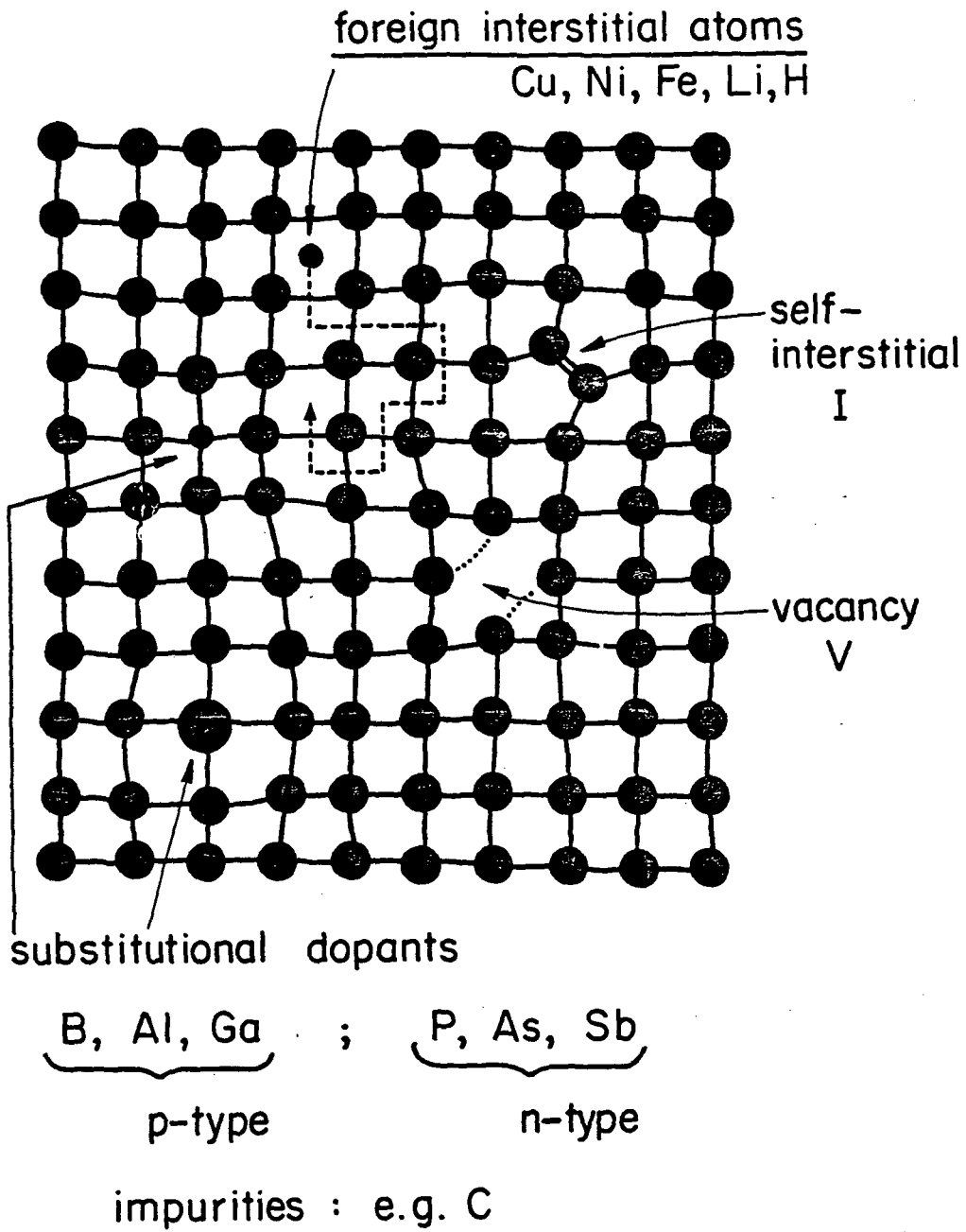


Fig. 2

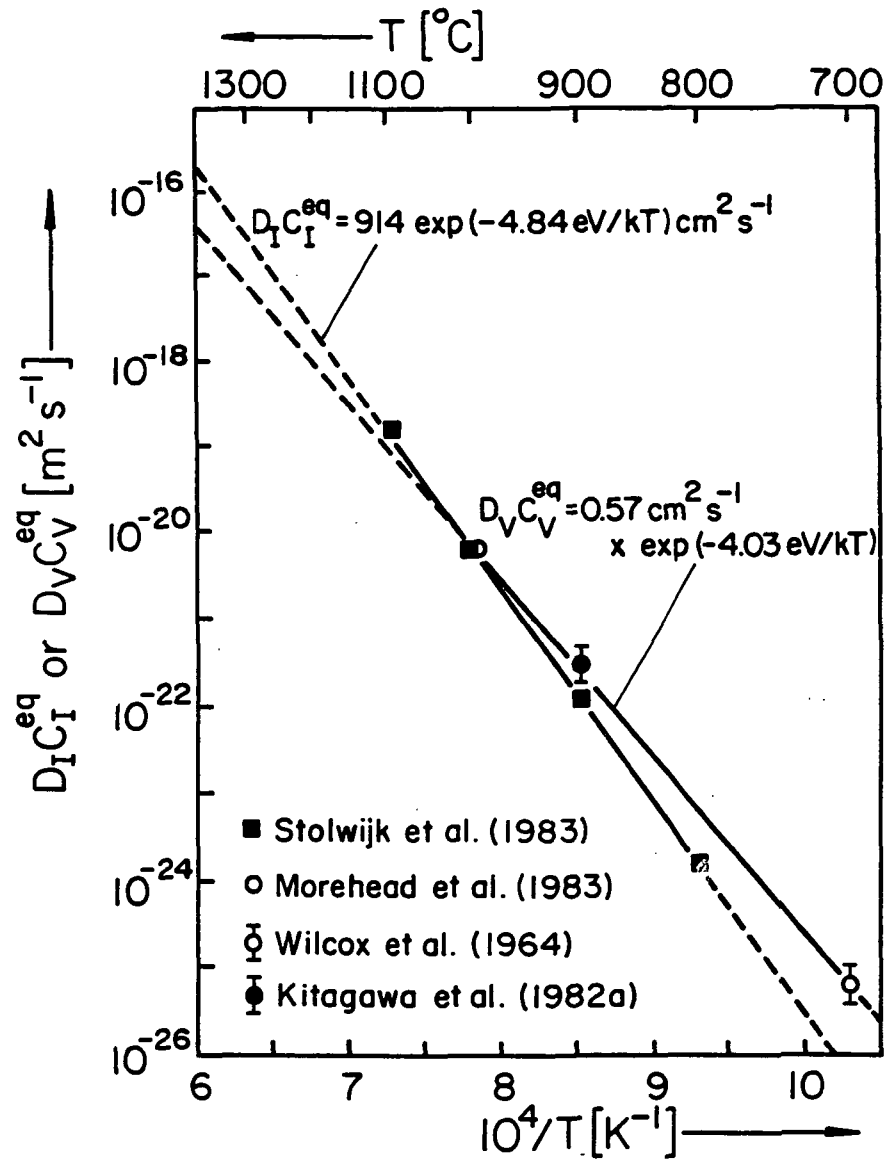


Fig. 3

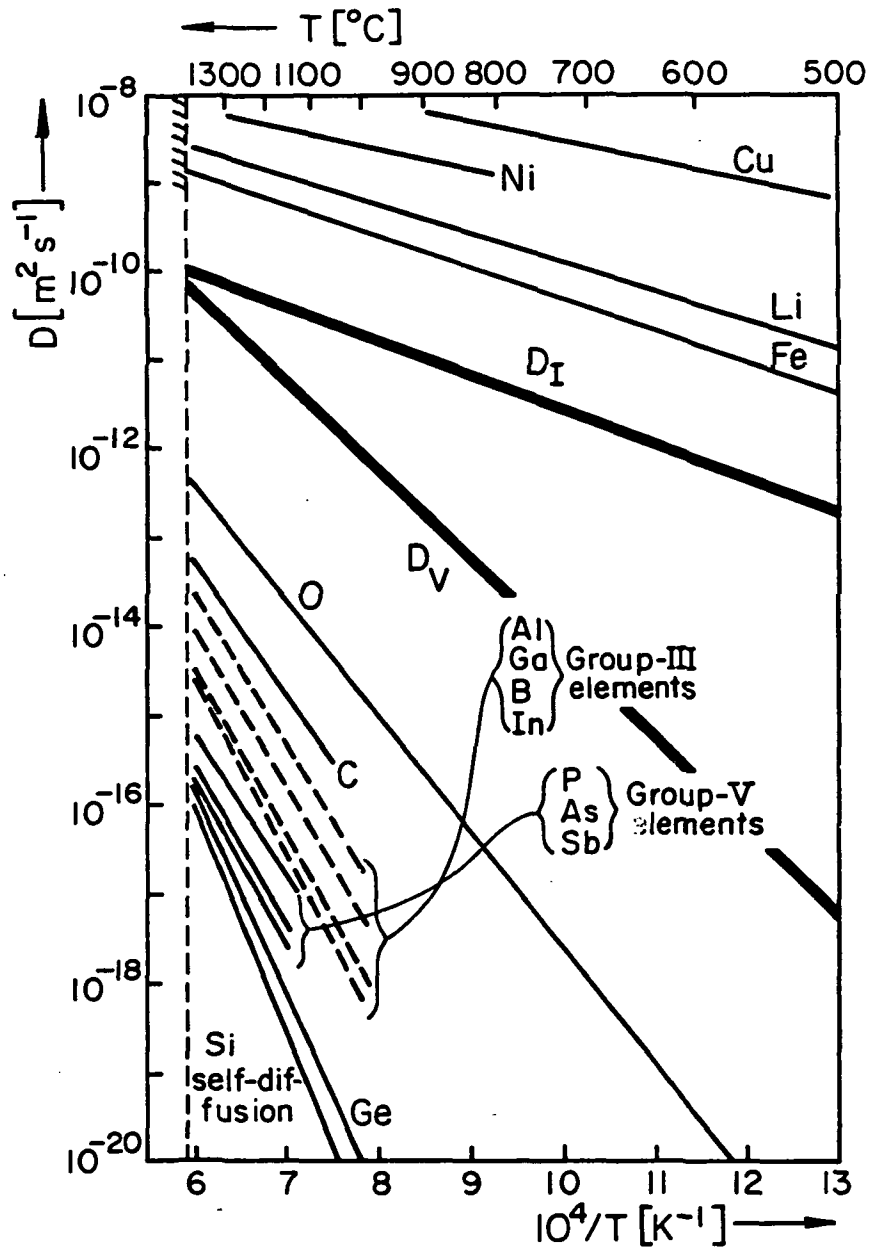


Fig. 4

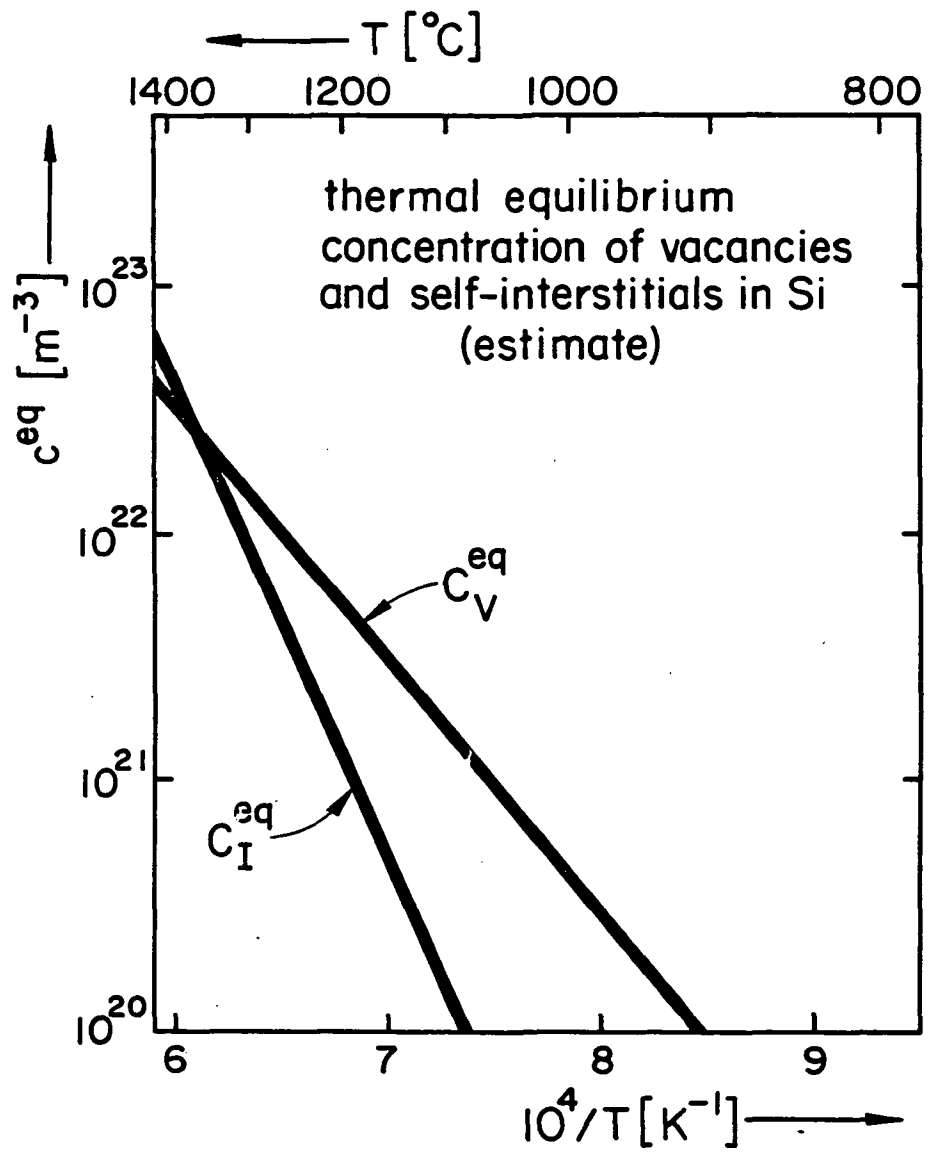


Fig. 5

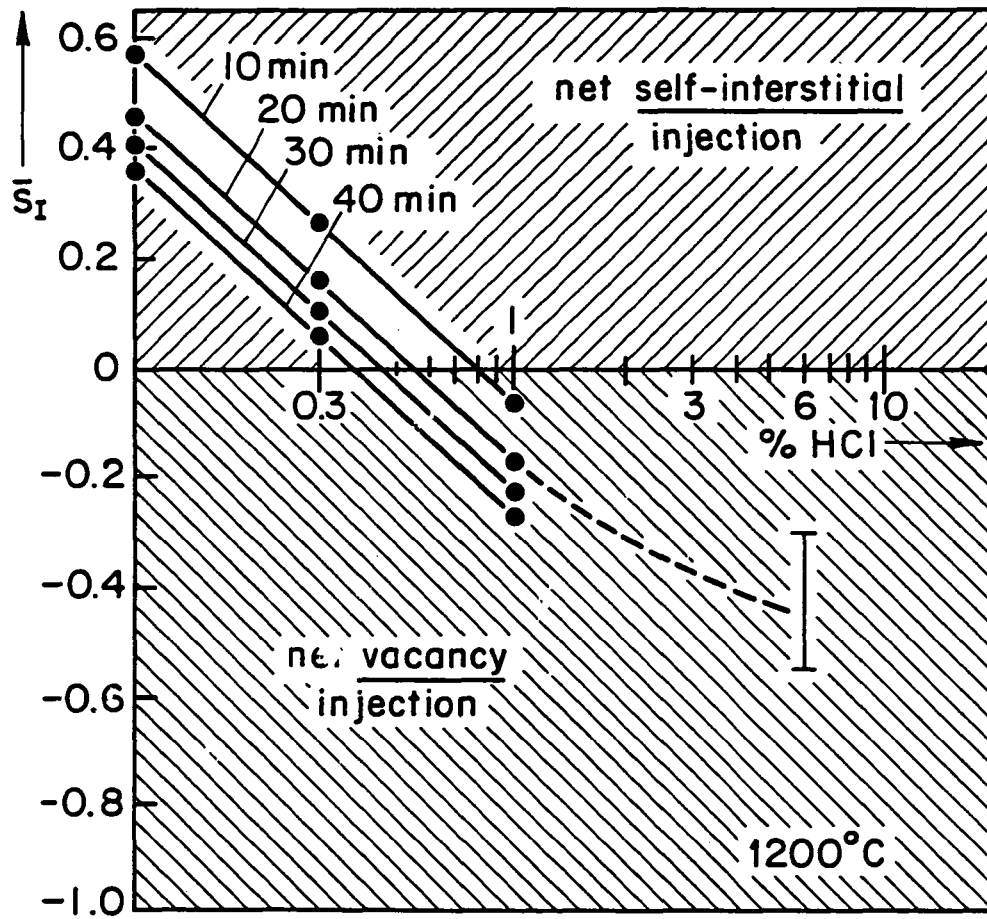


Fig. 6

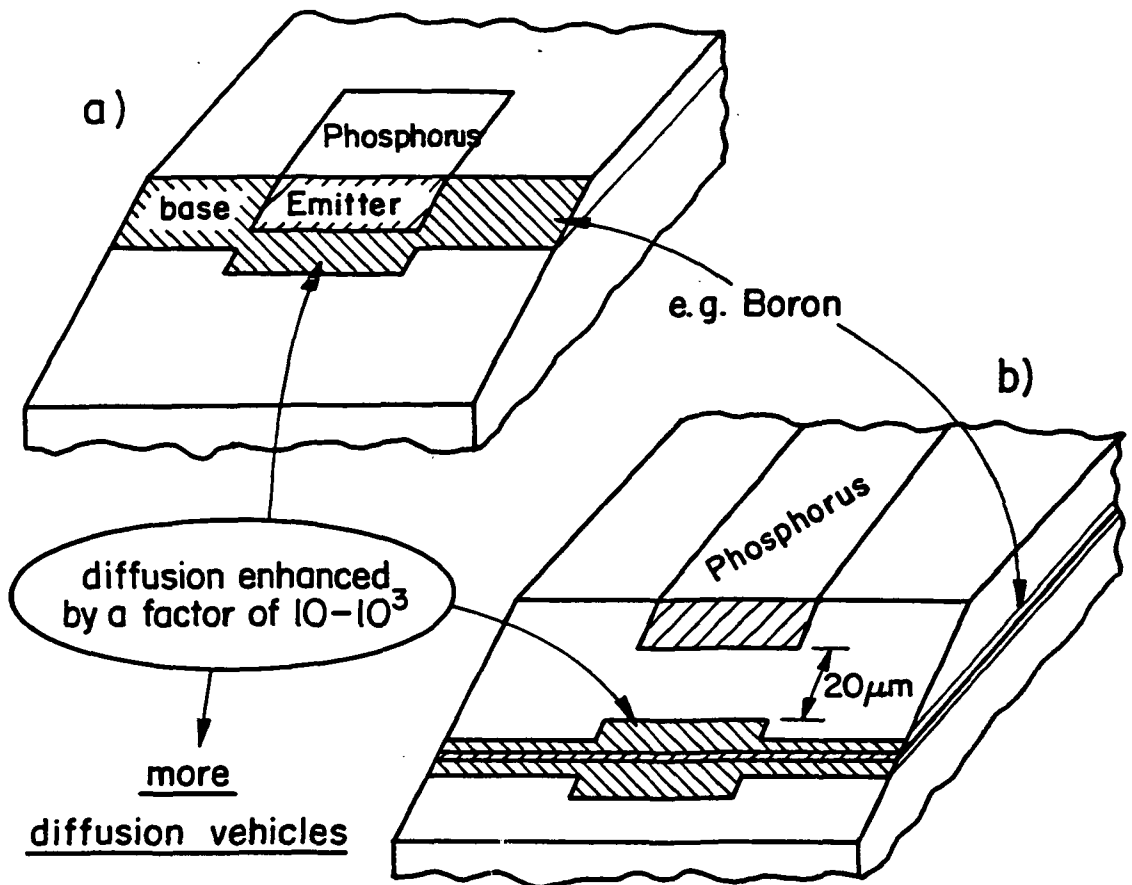
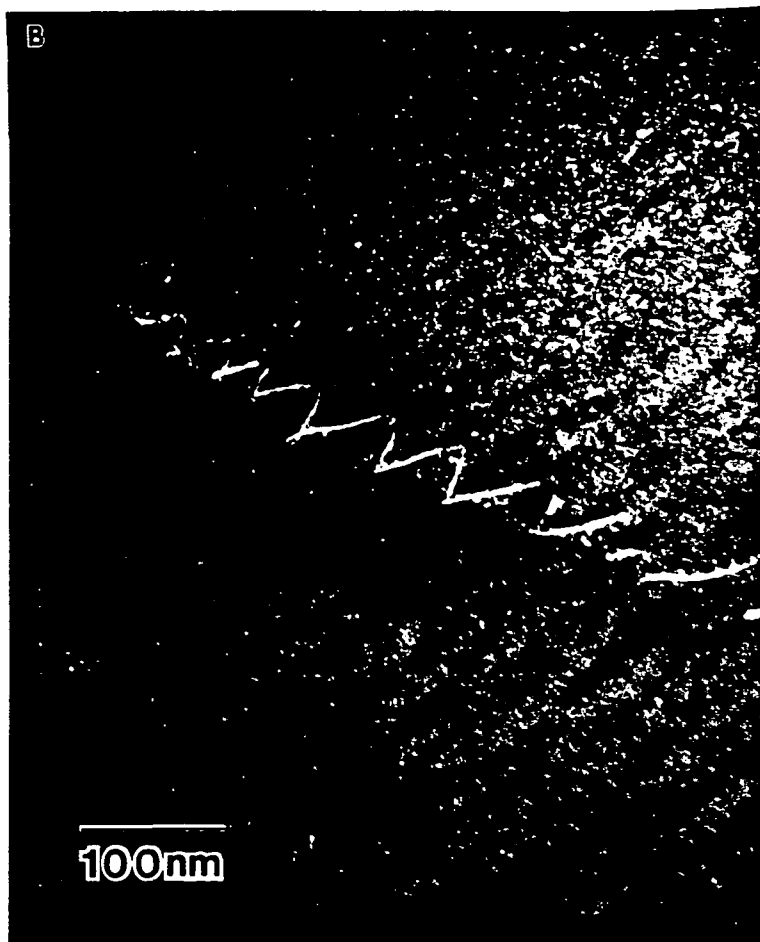


Fig. 7



*Fig. 8*

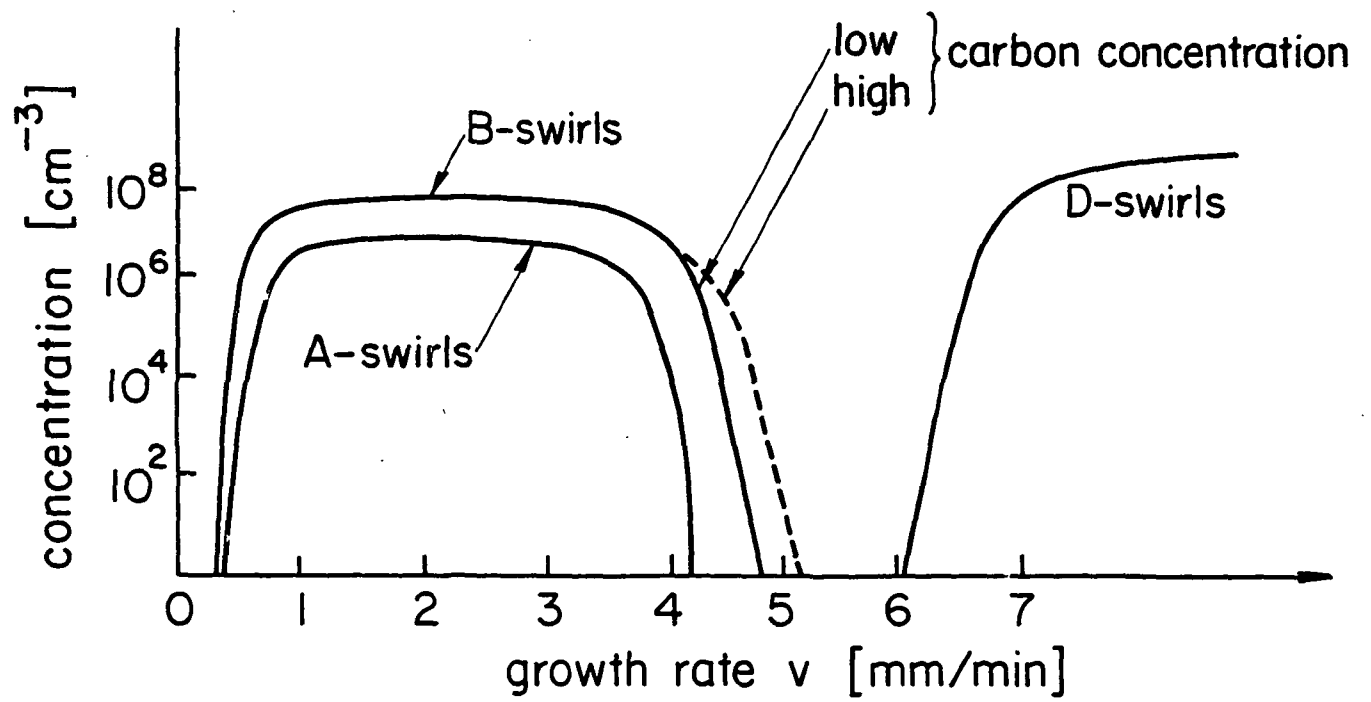


Fig. 9

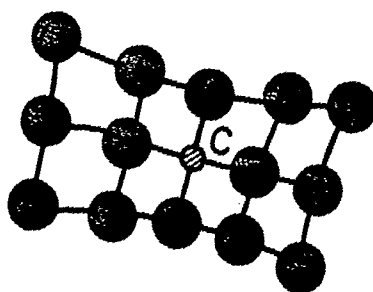


Fig. 10

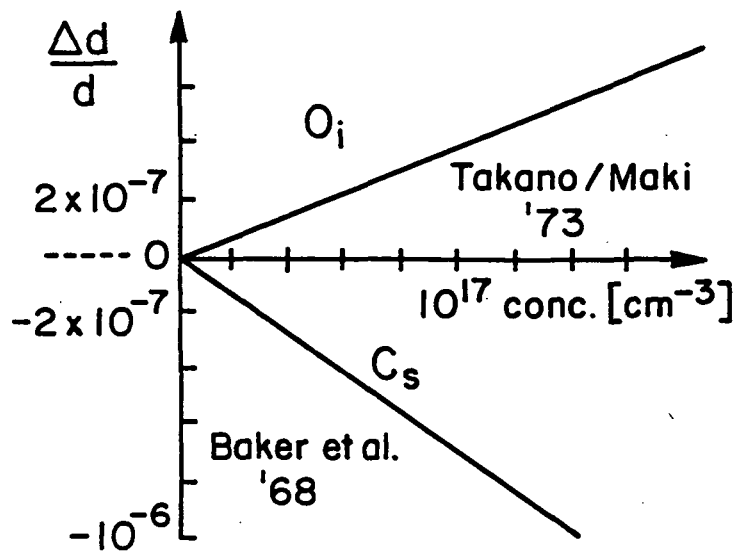


Fig. 11

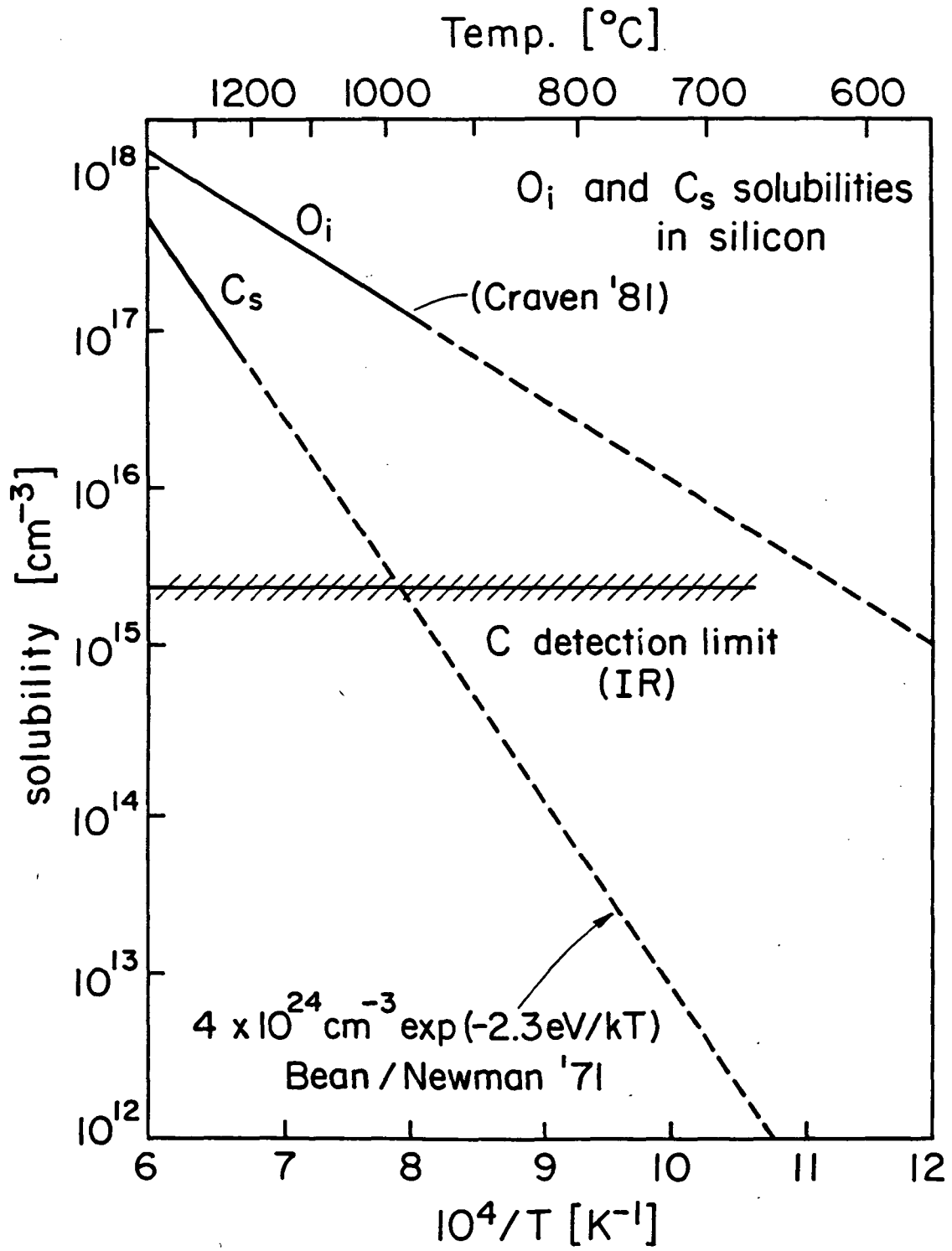


Fig. 12

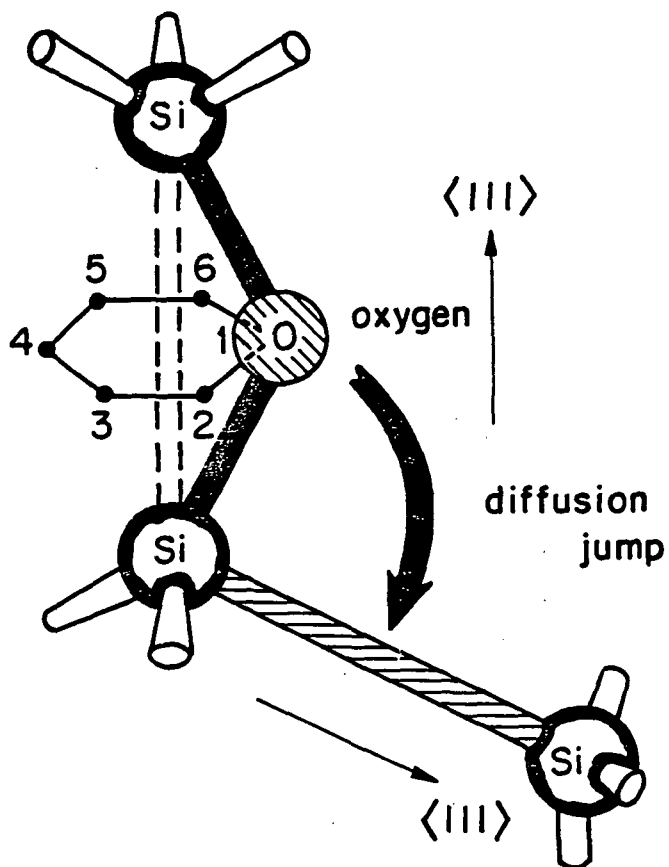


Fig. 13

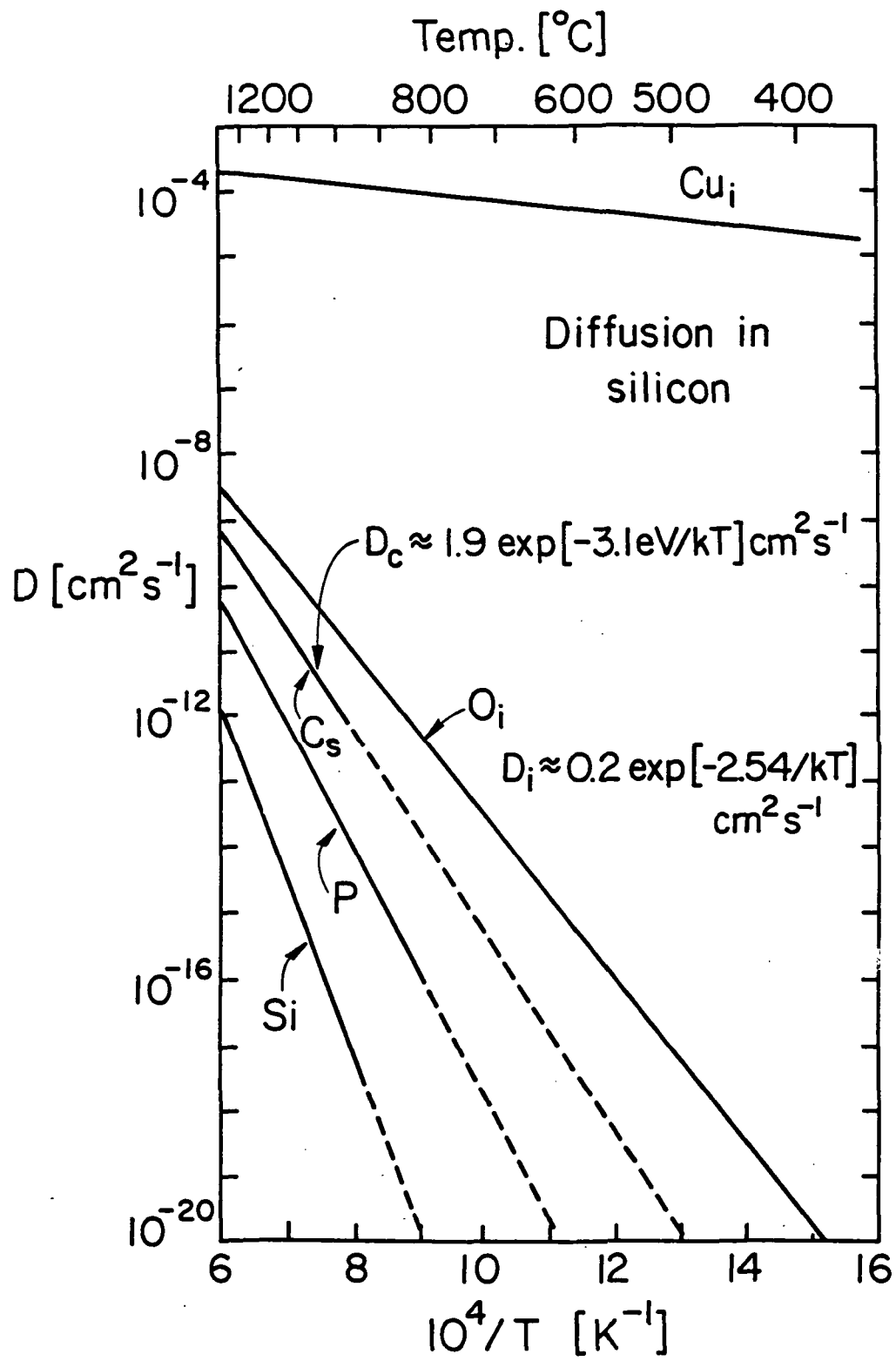
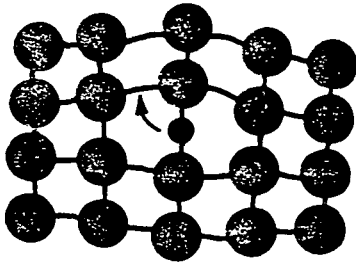


Fig. 14

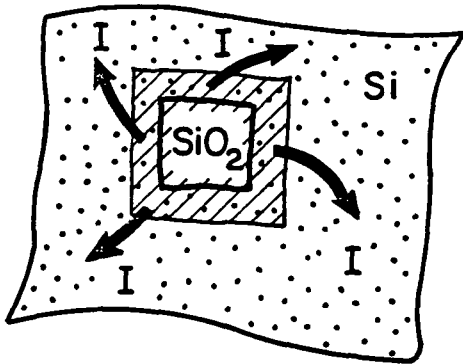


Oxygen

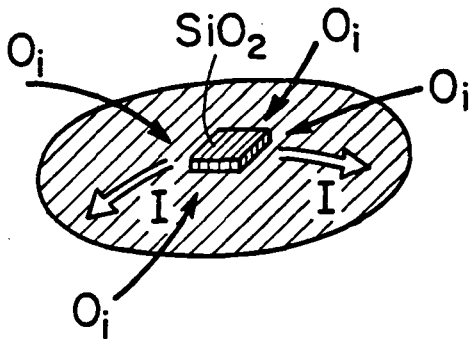


$\text{SiO}_2$

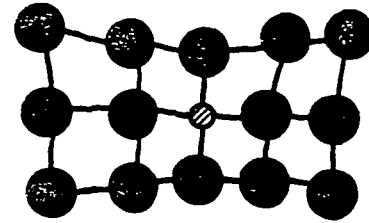
Volume increase  
(factor 2)



≈ I agglomerates

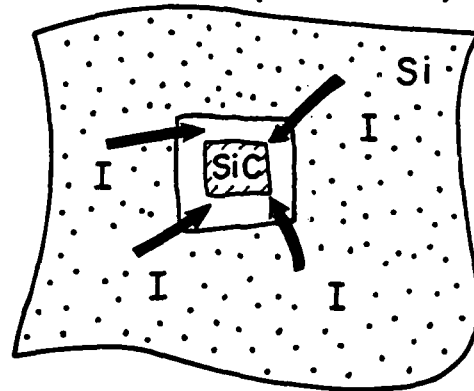


Carbon



$\text{SiC}$  or  
C agglomerate

Volume reduction  
(factor 2)



if I in supersaturation

≈ co-precipitation  
I and C

≈ "B-swirls"

Fig. 16

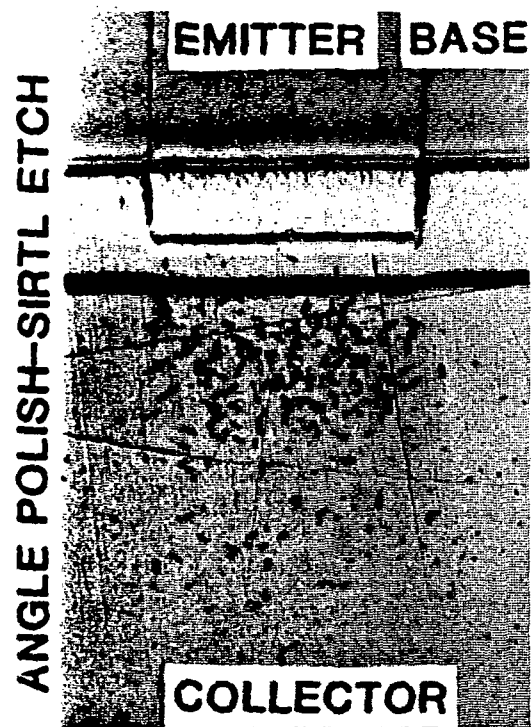


Fig. 17

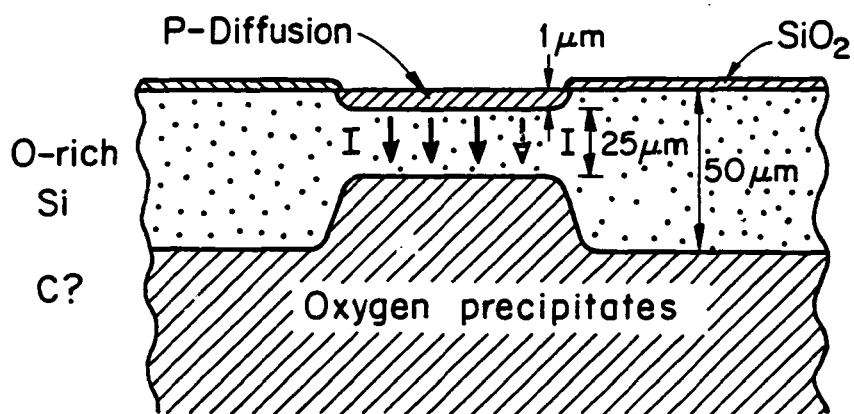
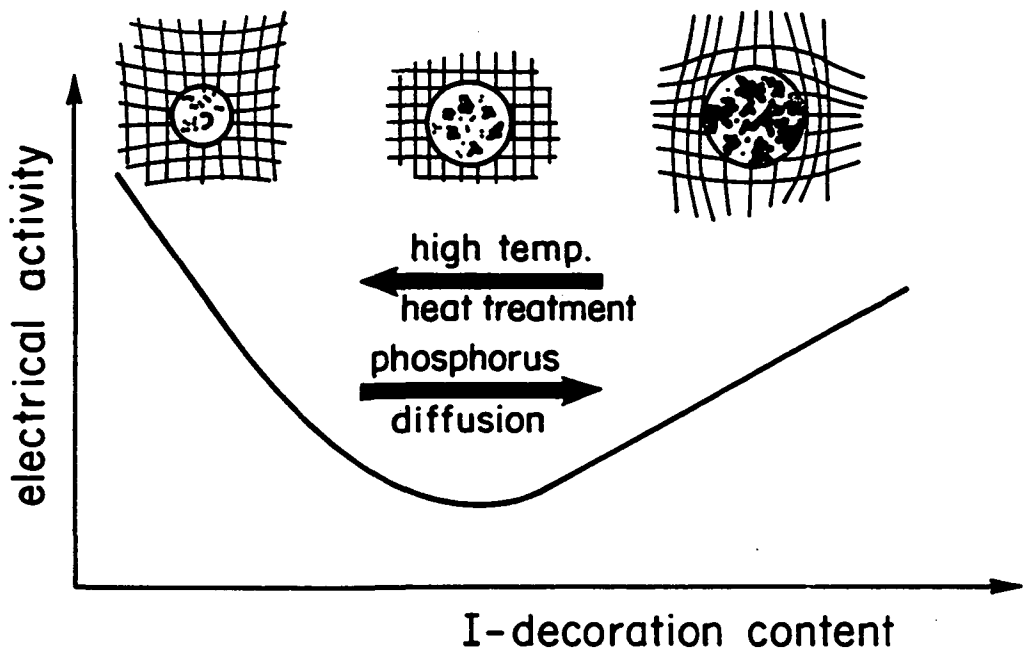


Fig. 18



*Fig. 19*